



# Mix design of concrete for prestressed concrete sleepers using blast furnace slag and steel fibers



Hyun-Oh Shin <sup>a</sup>, Jun-Mo Yang <sup>b</sup>, Young-Soo Yoon <sup>c,\*</sup>, Denis Mitchell <sup>a</sup>

<sup>a</sup> Department of Civil Engineering and Applied Mechanics, McGill University, 817 Sherbrooke Street West, Montreal, Quebec, H3A 0C3, Canada

<sup>b</sup> Energy-infra Research Group, Steel Solution Center, POSCO, POSCO Global R&D Center 100 Songdogwahak-ro, Yeonsu-gu, Incheon, 21985, Republic of Korea

<sup>c</sup> School of Civil, Environmental and Architectural Engineering, Korea University, 145 Anam-ro, Seongbuk-gu, Seoul, 02841, Republic of Korea

## ARTICLE INFO

### Article history:

Received 31 December 2015

Received in revised form

21 June 2016

Accepted 24 August 2016

Available online 30 August 2016

### Keywords:

Prestressed concrete sleeper

Ground granulated blast furnace slag

Steel fiber

Mix proportion

Mechanical property

Durability performance

## ABSTRACT

The application of ground granulated blast furnace slag (GGBFS) and steel fibers in prestressed concrete railway sleepers was investigated in this study. The use of GGBFS was considered as an eco-friendly material aimed at reducing CO<sub>2</sub> emissions and energy consumption as well as to enhance the durability performance of railway sleepers. Steel fibers improve the durability and structural performance in terms of crack control and reduction of spalling and can replace shear reinforcement. The mix proportions of the concrete incorporating GGBFS (56% GGBFS) and GGBFS with steel fibers (56% GGBFS and 0.75% steel fibers) were determined through a series of laboratory tests and a life cycle assessment. These mixes satisfied the requirements of the Korean Railway Standard and resulted in improved flexural capacity as well as less CO<sub>2</sub> emissions compared with current railway sleepers. Using these mixes, a total of ninety prestressed concrete sleepers were produced in a factory under the same manufacturing process as current railway sleepers, and their mechanical properties as well as durability performance were evaluated. The mix with partial replacement of Type III Portland cement by GGBFS showed an improved resistance to chloride ion penetration and freeze-thaw cycles compared with the concrete used for current railway sleepers. However, these mixes were more vulnerable to carbonation. The mix with GGBFS and steel fibers (mix BSF) showed a slightly better durability performance than the mix with GGBFS only (mix BS), including better carbonation and freeze-thaw resistances. The mix BSF showed decreased chloride ion penetration depth than mix BS but showed a slightly higher chloride ion diffusion coefficient.

© 2016 Elsevier Ltd. All rights reserved.

## 1. Introduction

Railway sleepers serve to transfer and distribute rail loads to the substructure supporting the rail, maintain the track gauge, and withstand the vertical and longitudinal movement of the rails [1–3]. Among the several types of railway sleepers, the demand for prestressed concrete sleepers is increasing for application in railway construction, especially for high-speed railway systems, due to the improved durability and structural performance as well as a reduced lifetime cost compared to timber or reinforced concrete sleepers [1–4]. However, some problems associated with prestressed concrete sleepers have been reported by previous studies

[3–5], such as the vulnerability to rail seat corrosion, susceptibility to chemical attack, their significant weight, and the high initial cost. There are increased concerns about the environmental effects of reinforced and prestressed concrete sleeper productions due to the fact that cement production consumes a large amount of energy and emits a considerable amount of carbon dioxide (CO<sub>2</sub>) (approximately 4–7% of the total global CO<sub>2</sub> emissions) that should be properly addressed [4–9]. Prestressed concrete sleepers are exposed to fatigue and impact loads as well as severe environmental conditions, resulting in cracks, spalling and deterioration of the sleepers. It is noted that rail seat deterioration, flexural cracks from center binding, and rail fastener failure are the three primary failure mechanisms of prestressed concrete sleepers [3,10]. These premature failures of railway sleepers prior to their anticipated lifetime lead to the replacement of 2–5% of damaged sleepers every year [4].

\* Corresponding author.

E-mail address: [ysyoon@korea.ac.kr](mailto:ysyoon@korea.ac.kr) (Y.-S. Yoon).

The use of ground granulated blast furnace slag (GGBFS) as a binder for concrete and the addition of steel fibers in concrete mixes can be used to address the aforementioned problems of current railway sleepers. GGBFS, an industrial by-product material generated from the manufacturing of pig iron, is well known for its high long-term strength and resistance to deterioration under severe environmental conditions as well as its environmental advantages due to lower CO<sub>2</sub> emissions and energy consumption [11–13]. It is found that GGBFS can reduce concrete CO<sub>2</sub> emissions by 22% in typical concrete mixes [8,9]. Previous research [6,14] has considered GGBFS as a binder of concrete mix for railway sleeper applications, but it should be noted that the replacement ratio of GGBFS is limited (30%), with alkaline solution being added to these concrete mixes to improve the mechanical and durability performance. Numerous studies have shown that the addition of steel fibers can reduce and delay concrete spalling, control the initiation and growth of cracks, and offer impact resistance and durability [15]. Recent research [16–19] showed that steel fibers can even partially substitute for confinement reinforcement in columns as well as stirrups in beams. The use of steel fibers in beams without transverse reinforcement can enhance the shear resistance and ductility.

These combined benefits of GGBFS and steel fibers are being investigated as possible solutions to the structural and durability issues of current prestressed concrete sleepers. The following steps were taken to investigate the application of GGBFS and steel fibers in prestressed concrete sleepers: 1) selecting appropriate mix proportions of the concrete, with partial substitution of GGBFS and application of steel fibers (Section 2); 2) the production of prototype prestressed concrete sleepers under the same production process used for current railway sleepers (Section 3); and 3) the evaluation of their mechanical properties and durability performance (Sections 3 and 4) including comparisons with current prestressed concrete sleepers.

## 2. Selecting mix proportions

### 2.1. Determination of GGBFS replacement ratio

#### 2.1.1. Current code requirements and trial batches

Prestressed concrete sleepers are a precast concrete product, therefore, they are produced in a factory. To achieve a daily production cycle, the concrete must reach a strength sufficient to permit release of the pretensioned strands in about 16 h [20]. The Korean Railway Standard (KRS TR 0008) [21] specifies a minimum initial compressive strength of concrete (35 MPa) and it requires the use of Type III Portland cement (high early strength cement) for prestressed concrete production to address early-age strength required for stand release. It further requires the use of steam curing or heating to obtain a sufficient early-age strength for strand release. Table 1 summarizes the requirements for prestressed concrete sleepers in the Korean Railway Standard (KRS TR 0008) [21] and in the manufacturing guideline [22]. Numerous trial batches were made and tested to determine the most appropriate mix design of the concrete incorporating GGBFS and steel fibers. As a result, the preliminary mix proportions for slag concrete (“BS-control” in Table 2) were determined [23]. This preliminary slag concrete mix was designed to have a lower water-binder ratio (w/b) and a higher unit water amount compared to the conventional concrete mix (“CC” in Table 2) for current prestressed concrete sleeper production to achieve appropriate initial concrete strength and workability considering the application of GGBFS and steel fibers in the mix.

#### 2.1.2. Experimental design, mix proportions and materials

Based on pre-determined preliminary mix, the weight ratios of 42, 49, and 56% of Type III Portland cement were replaced by GGBFS in order to determine an appropriate mixing ratio for prestressed concrete sleepers with slag. Each mix was designated as BS42, BS49, and BS56 based on their slag replacement ratio. Details of the concrete mix proportions for the testing (BS-series), as well as the reference concrete mix for current railway sleepers (mix CC) are shown in Table 2. Appropriate mix proportions of the concrete with GGBFS (GGBFS replacement ratio) were determined by a series of tests to satisfy the target slump, compressive strength at early-age (16 h) and at 28 days, and by comparing the amount of CO<sub>2</sub> emissions of the concrete with different mix proportions. The material properties of GGBFS and Type III Portland cement, which were specified by the manufacturer, are presented in Table 3. The same coarse aggregate with a maximum size of 20 mm and specific gravity of 2.61 and fine aggregate with specific gravity of 2.41 were used for all mixes. A polycarboxylic acid based water reducing admixture was incorporated into the BS-series mixes as well as mix CC, in solution form to attain the required workability.

#### 2.1.3. Curing

The Korean Railway Standard [21] specifies two different curing methods for compressive test specimens: 1) steam curing of the specimens to verify strength at demolding or strand release (about 16 h); and 2) moisture curing of the specimens to check the specified design concrete strength at 28 days. After concrete casting, six 100 mm diameter by 200 mm concrete cylinders were cured in a steam curing chamber and another six cylinders were cured in water tanks. Steam curing was performed according to the temperature hysteresis in KRS TR 0008 [21] (see Table 1 and Fig. 1(a)). The curing regime consisted of 3 h at ambient temperature after casting, followed by 2 h of temperature rise at a rate of 15 °C/h up to a maximum temperature of 50 °C. This maximum temperature was maintained for 5 h, and then the temperature dropped to ambient temperature at a rate of 10 °C/h. After 3 h of curing at ambient temperature, the specimens were tested to determine the concrete strength for strand release. It is noted that this curing regime was chosen to avoid the delayed ettringite formation according to the Portland Cement Association (PCA) recommendations (i.e., preset curing, rates of temperature rise and decrease, and the maximum temperature) [24]. It is also noted that this temperature regime was the same as the steam curing method for the current production of prestressed concrete sleepers. The cylinders for the specified compressive strength test were removed from the molds 24 h after concrete casting and then, they were cured in a water storage tanks (moisture curing) in a temperature range of 20–23 °C (see Fig. 1(b)) for 27 days, resulting in a total of 28 days of moisture curing.

#### 2.1.4. Workability and compressive strength

The slump test was carried out in accordance with ASTM C143/C143M [25] for each batch of concrete. The compressive strengths at 16 h after steam curing and 28 days of moist curing were measured by six concrete cylinders for each type of curing regime in accordance with ASTM C39/C39M [26].

Table 4 summarizes the test results of mixes incorporating different amount of GGBFS. All mixes with GGBFS (BS-series) showed at least 80 mm of slump, satisfying workability requirements for casting and also achieving the target slump values specified in Table 1. It is noted that 0.9–1.0% of water reducing admixtures by weight of the binder were added to all mixes to achieve the required workability. Concrete mixes for current railway sleepers with Type III Portland cement (mix CC) also showed sufficient workability with a slump of 75 mm. Table 4 shows the compressive strength test results at 16 h and at 28 days. At 16 h,

**Table 1**  
Concrete requirements for railway sleepers.

| Item                | Detailed item   | Requirement   | Remark                |
|---------------------|---|---|-----------------------|
| Material            | Maximum coarse aggregate size ( $G_{max}$ )             | 20 mm, high durability  |                       |
| Mix and fabrication | Cement  | Type III – High early strength concrete (<440 kg/m <sup>3</sup> )   |                       |
|                     | Water-cement ratio                                      | Maximum 35%   |                       |
|                     | Air content   | 3.5 ± 1.5%  |                       |
| Curing              | Slump   | Reasonable value for concrete casting (about 80 ± 25 mm) <sup>a</sup>   |                       |
|                     | Placement concrete                                      | Within one hour   |                       |
|                     | Steam curing or Heat curing                             | - Start: more than two hours after placement of concrete<br>- Rising Temperature: <15 °C/h<br>- Dropping Temperature: <10 °C/h<br>- Maximum Temperature: <60 °C |                       |
| Strength            | At release of the strand (About 16 h)                   | >35 MPa (KRS T0008-11)<br>>30 MPa (KRS T0008-15)  | Under steam curing    |
|                     | Specified compressive strength of concrete (At 28 days) | Higher than specified strength in the product requirement (>about 50 MPa) <sup>a</sup>  | Under moisture curing |

<sup>a</sup> Required values specified in manufacturing guideline for current prestressed concrete sleepers [22].

**Table 2**  
Preliminary concrete mix proportions.

| Mix        | W/B [%] | S/a [%] | Unit weight [kg/m <sup>3</sup> ] |  |       |      |        | AD [%]  | Remarks (test or not)    |
|------------|---------|---------|----------------------------------|--|-------|------|--------|---------|--------------------------|
|            |         |         | Water                            | Cement (III)                                   | GGBFS | Sand | Gravel |         |                          |
| CC         | 32.3    | 44.7    | 134                              | 415  | –     | 814  | 1006   | 0.9     | Reference – tested       |
| BS-control | 30.0    | 44.7    | 147                              | Total binder = 490<br>(Amount of GGBFS varied) |       | 764  | 943    | varying | Control mix – not tested |
| BS42       |         |         |                                  | 284  | 206   |      |        | 0.9     | Variable – tested        |
| BS49       |         |         |                                  | 250  | 240   |      |        | 1.0     | Variable – tested        |
| BS56       |         |         |                                  | 216  | 274   |      |        | 1.0     | Variable – tested        |

W/B: water-binder ratio, S/a: sand-to-aggregate ratio, Cement (III): Type III Portland cement – high early strength cement, GGBFS: ground granulated blast furnace slag, and AD: polycarboxylic acid based water reducing admixture.

**Table 3**  
Physical properties and chemical composition of cement and GGBFS.

| Type           | Physical properties |                               |                  | Chemical compositions |                                |                                |      |     |                  |                  |                  |  |
|----------------|---------------------|-------------------------------|------------------|-----------------------|--------------------------------|--------------------------------|------|-----|------------------|------------------|------------------|--|
|                | Specific gravity    | Fineness (cm <sup>2</sup> /g) | Loss on ignition | SiO <sub>2</sub>      | Al <sub>2</sub> O <sub>3</sub> | Fe <sub>2</sub> O <sub>3</sub> | CaO  | MgO | C <sub>3</sub> S | C <sub>2</sub> S | C <sub>3</sub> A |  |
| OPC (Type III) | 3.15                | 3415                          | 1.19             | 20.0                  | 4.8                            | 3.4                            | 62.2 | 3.5 | 56.2             | 15.0             | 6.8              |  |
| GGBFS          | 2.90                | 4448                          | 0.30             | 34.5                  | 12.7                           | 0.50                           | 41.3 | 5.9 | –                | –                | –                |  |

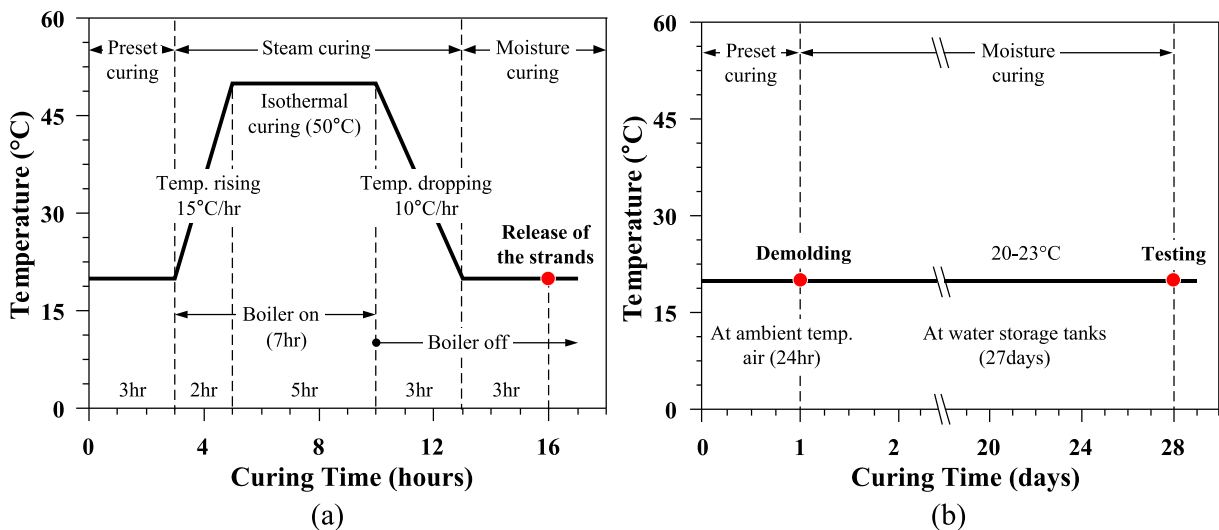


**Fig. 1.** Temperature variation during curing: (a) steam curing; (b) moist curing.

specimens that were produced using the BS-series mixes had an average compressive strength of 50.8 MPa, varying from 48.8 to

52.4 MPa. These strengths were lower than that of mix CC; however, they are significantly higher than the strength requirement for

**Table 4**  
Slump, compressive strength and CO<sub>2</sub> emissions.

| Mix  | Slump [mm]<br>(>60 mm) | Compressive strength [MPa]     |                                  | CO <sub>2</sub> emission [Kg-CO <sub>2</sub> /m <sup>3</sup> ] |  |                           |
|------|------------------------|--------------------------------|----------------------------------|--|--|---------------------------|
|      |                        | At 16 h <sup>a</sup> (>35 MPa) | At 28 day <sup>b</sup> (>50 MPa) | Material phase (CO <sub>2-M</sub> )                            | Production phases (CO <sub>2-P</sub> ) | Total (%) <sup>c</sup>    |
| CC   | 75                     | 54.2 (1.58) <sup>d</sup>       | 72.1 (4.79) <sup>d</sup>         | 398.5  | 175.0                                  | 573.5 (100%) <sup>c</sup> |
| BS42 | 80                     | 48.8 (1.27)                    | 67.5 (3.74)                      | 318.4  | 175.0                                  | 493.4 (86%)               |
| BS49 | 85                     | 51.9 (0.89)                    | 65.9 (3.54)                      | 292.6  | 175.0                                  | 467.6 (82%)               |
| BS56 | 80                     | 52.4 (1.20)                    | 68.9 (5.87)                      | 267.6  | 175.0                                  | 442.6 (77%)               |

<sup>a</sup> Testing performed after steam curing.

<sup>b</sup> Testing performed after moisture curing.

<sup>c</sup> The ratio of total CO<sub>2</sub> emission of each mix to total CO<sub>2</sub> emission of mix CC.

<sup>d</sup> Items in parentheses ( ) = standard deviation.

the strands release in KRS TR 0008 [21]. Mix CC showed higher strength compared to the BS-series at 28 days as well, but the compressive strengths of all mixes were 16–22 MPa higher than the target compressive strength. Test results also indicated that the effects of the replacement ratio of GGBFS on the compressive strength were not significant. All mixes, both CC- and BS-series, reached approximately 75% of the 28-day compressive strength at 16 h by steam curing, which is 15–30% higher than the early-age strength of the moist-cured concrete. This result clearly demonstrates the benefits of steam curing on the early-age strength of concrete for the strands release. The test results of previous studies [27,28] also support this finding. These studies showed that the ratios of the one-day strength after hot temperature curing (60 °C and 40 °C) to the 28-day strength after moist curing (20 °C) ranged from roughly 45–70%, which were much higher than the ratios of typical moist curing. These results were somewhat lower than the result observed in this study; however, this can be explained by the benefits of steam versus heat curing, and the difference of the temperature regimes as well as the use of Type III Portland cement in this study.

### 2.1.5. Comparison of CO<sub>2</sub> emissions

All mixes produced with partial substitution of GGBFS for Type III Portland cement showed sufficient workability, sufficient strength for strand release as well as specified compressive strength at 28 days, regardless of the replacement ratio of GGBFS. It is well known that using GGBFS reduces CO<sub>2</sub> emission for concrete production, therefore, the level of CO<sub>2</sub> emission could be another critical factor in assessing the appropriate mix proportions.

A life cycle assessment (LCA) was carried out to estimate CO<sub>2</sub> emissions for prestressed concrete sleepers considering different substitution levels of GGBFS. The LCA approaches used in this study were adapted from Yang and et al. [8,29] and Won et al. [13] which followed procedures described by the International Organization for Standards (ISO) 14040 [30]. Yang et al. [8,29] proposed an approach for the calculation of a total CO<sub>2</sub> emission,  $C_e$ , for 1 m<sup>3</sup> concrete that is based on the individual integration method:

$$C_e = CO_{2-M} + CO_{2-T} + CO_{2-P} \quad (1)$$

where,  $CO_{2-M}$ ,  $CO_{2-T}$ ,  $CO_{2-P}$  represent the CO<sub>2</sub> emissions from the raw material phases, transportation phases, and concrete production phases, respectively. Yang et al. [8,29] reported that the ratios of CO<sub>2</sub> emissions from  $CO_{2-M}$ ,  $CO_{2-T}$ , and  $CO_{2-P}$  for typical concrete production, with a compressive strength of 35 MPa, are approximately 87, 5, and 8%, respectively. The portion of  $CO_{2-T}$  is relatively small compared to that from the other phases and the portion of  $CO_{2-T}$  for prestressed concrete sleepers, which are typically produced in a factory, can be decreased since  $CO_{2-T}$  includes the CO<sub>2</sub> inventory of the in-transit mixing truck for fresh concrete. Therefore, the amount of CO<sub>2</sub> emissions from the transportation phases

( $CO_{2-T}$ ) was neglected in this study. The Korean Life Cycle Inventory (LCI) database [7] was used to estimate the amount of CO<sub>2</sub> emissions for the raw material phases ( $CO_{2-M}$ ). Although the test specimens were cured in a laboratory steam curing chamber, the amount of CO<sub>2</sub> emissions for the production phases were evaluated by assuming steam curing conditions of the current railway sleepers production process. That is, the amount of CO<sub>2</sub> emissions for the production phases were mainly evaluated from the CO<sub>2</sub> emissions due to the oil that is used in the boiler for the steam curing [13,31]. Example calculations of CO<sub>2</sub> emissions for the mixes CC and BS56 is presented in Table 5 and the results of CO<sub>2</sub> emissions for all mixes are presented and compared in Table 4.

The amount of CO<sub>2</sub> emissions per unit volume of slag concrete (BS-series) ranged from approximately 77–86% of that of the concrete for conventional railway sleepers (mix CC). This result indicated that the partial substitution of GGBFS for Type III Portland cement significantly decreases CO<sub>2</sub> emissions of the concrete. The reduction of CO<sub>2</sub> emissions increases with increasing GGBFS replacement ratio.

The results described above demonstrate that mixes produced with partial substitution of GGBFS for Type III Portland cement showed sufficient workability and strengths for strand release at early-age as well as the specified compressive strength at 28 days. Furthermore, they also satisfied all requirements for prestressed concrete sleepers specified in KRS TR 0008 [21]. The LCA results indicated that mix BS56 had the lowest CO<sub>2</sub> emission per unit volume, which is 27% (131 kg-CO<sub>2</sub>/m<sup>3</sup>) lower than that for the concrete currently used in railway sleepers. Therefore, mix BS56 was selected as the concrete mix for eco-friendly railway sleepers and this mix was used for the subsequent test series.

### 2.2. Steel fiber content

The addition of steel fibers can improve the mechanical and durability performance of prestressed concrete sleepers. However, high volume fractions of fibers can have a negative effect due to “balling” of the fibers. Furthermore, the addition of steel fibers can increase the total cost of manufacturing sleepers [32]. Therefore, the ideal amount of steel fibers, considering performance and economics, should be determined.

To determine the most appropriate steel fiber content for slag concrete mix, the flexural performance of slag concrete with varying steel fiber content was mainly investigated. Flexural performance under static loading such as flexural strength and toughness as well as flexural performance under impact loading, such as dissipated energy, are well-known indicators that illustrate the beneficial effect of steel fibers [32,33]. Therefore, both static and impact loading tests were carried out in this study. The slump of fresh concrete and the compressive strength of hardened concrete with different volume fractions of steel fibers were also investigated.

**Table 5**  
Example calculations of CO<sub>2</sub> emissions.

| Raw material phase (CO <sub>2-M</sub> )     | CO <sub>2</sub> emission of materials [kg-CO <sub>2</sub> /kg]                    | Unit weight of materials [kg/m <sup>3</sup> ]           |                         | CO <sub>2</sub> emission of concrete [kg-CO <sub>2</sub> /m <sup>3</sup> ] |                      |
|---|---|---|-------------------------|--|----------------------|
|   |   | CC  | BS56                    | CC   | BS56                 |
| Materials                                   |   |   |                         |  |                      |
| Cement                                      | 0.94  | 415   | 216                     | 391.8  | 203.9                |
| Slag cement (GGBFS)                         | 0.21  | –   | 274                     | –  | 57.0                 |
| fine aggregate                              | $1.60 \times 10^{-3}$   | 814   | 764                     | 1.3  | 1.2                  |
| coarse aggregate                            | $4.30 \times 10^{-3}$   | 1006  | 943                     | 4.4  | 4.1                  |
| Water                                       | $1.96 \times 10^{-4}$   | 134   | 147                     | $2.6 \times 10^{-2}$   | $2.9 \times 10^{-2}$ |
| Admixture                                   | 0.25  | 4.15  | 5.38                    | 1.0  | 1.3                  |
| Sub Total (CO <sub>2-M</sub> )              | CO <sub>2</sub> emission at raw material phase                                    |   |                         | 398.5  | 267.6                |
| <b>Production phases (CO<sub>2-P</sub>)</b> | Use of oil for curing   | Temperature rising (2 h)                                | Isothermal curing (5 h) | CO <sub>2</sub> emission of concrete [kg-CO <sub>2</sub> /m <sup>3</sup> ] |                      |
|   |   |   |                         | CC   | BS56                 |
| Calculation                                 | 2.5 kg-CO <sub>2</sub> /L 10 L-oil/hr   | (2.5 kg-CO <sub>2</sub> /L × 10 L/hr) × (2 + 5 h) = 175 |                         | 175.0  | 175.0                |
| Sub Total (CO <sub>2-P</sub> )              | CO <sub>2</sub> emission at production phase                                      |   |                         | 175.0  | 175.0                |
| <b>Total (C<sub>e</sub>)</b>                | CO <sub>2</sub> emission for the sleeper (CO <sub>2-M</sub> + CO <sub>2-P</sub> ) |   |                         | 573.5  | 442.6                |

2.2.1. Test variables, mix proportions and materials

Mix BS56 which was presented in Section 2.1 was used for all batches and only the steel fiber volume fractions ( $v_f = 0, 0.25, 0.5, 0.75$  and  $1.0\%$ ) were varied. Each mix was identified as BSF0, BSF0.25, BSF0.5, BSF0.75, and BSF1.0 according to the steel fiber content. Bundled-type hooked-end steel fibers with a length of 30 mm and a diameter of 0.5 mm, resulting in an aspect-ratio ( $l/d$ ) of 60, were used in this study. The density, tensile strength, and elastic modulus of this steel fibers, according to the information given by the manufacturer, are 7.85 kg/m<sup>3</sup>, 1100 MPa, and 200 GPa, respectively.

2.2.2. Test setup and procedure

The compression test at 28 days and the slump test of fiber-reinforced slag concrete were carried out as described in Section 2.1.4. In order to investigate the flexural capacity, six prismatic specimens (100 × 100 × 400 mm) for each mixture were cast and each set of three specimens was tested under different loading conditions: 1) third-point static loading in accordance with ASTM

C1609/1606M [34] by using a 2500 kN capacity universal testing machine (see Fig. 2(a)); and 2) low-velocity impact loading by using a drop weight impact machine (see Fig. 2(b)). A load cell with a 250 kN capacity was used to measure the applied load and two linear variable differential transducers (LVDTs) were used to measure the mid-span deflection of the beam specimens in static flexural tests. An impact load with a potential energy of 300 J and an incident impact velocity of 3.66 m/s was applied to the mid-length of the beams, and the loads and velocities were measured using a load cell and speedometer installed in the drop weight. The deflection at the mid-span was measured by a high-speed laser displacement sensor in the impact test. The same support with a 300 mm clear span length was used for both the static and impact flexural tests. The moist curing method described in Section 2.1.2 was used for all specimens and they were tested at 28 days.

2.2.3. Test results and steel fiber content

Fig. 3(a) summarizes slump and compressive strength test results of the fiber-reinforced slag concrete, including the amount of water reducing admixture that is used in the mixes. The higher amounts of water reducing admixture, 1.1–1.2% by weight of the binder, were used for the mixes containing steel fibers to improve workability due to the fact that the addition of steel fibers decreases the slump of the concrete. The slag concrete mix with 0.25% steel fibers acquired the same slump as the mix without steel fibers by using a 1.1% water reducing admixture. Although a higher amount of water reducing admixture was used for concrete mixes with 0.5–1.0% steel fibers less slump of the mix with higher fiber volume fraction was achieved. Nevertheless, slag concrete mixes with 0.5 and 0.75% steel fibers showed sufficient workability for casting and the slump test results satisfied the target slump value specified in Table 1. The slag concrete mix with 1.0% fiber volume fraction showed the lowest slump value of 30 mm which was not sufficient for concrete casting. The slag concrete mixes with more than 1.2% of water reducing admixtures exhibited aggregate separation, therefore, 1.2% of water reducing admixture was considered to be the upper limit.

The compressive strength of the concrete with 0.25% steel fibers was slightly lower than the concrete without steel fibers, but it increased for concrete with a fiber content of 0.5%. The highest compressive strength was obtained in concrete with 0.5% steel fibers, but the compressive strength reduced with further increases in steel fiber ratio to 0.75 and 1.0%. The variation of compressive strength as a function of fiber volume fraction was not significant in this study and all mixes achieved sufficient compressive strength in

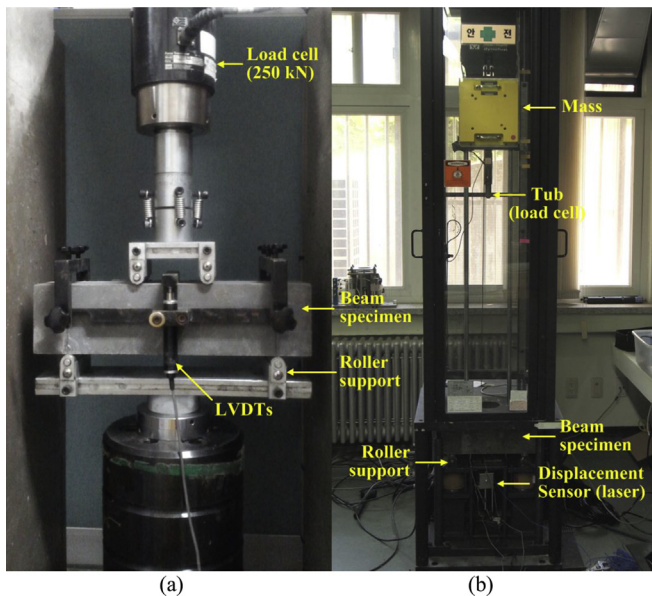


**Fig. 2.** Flexural test setups: (a) third point flexure test (static); (b) drop weight impact test.

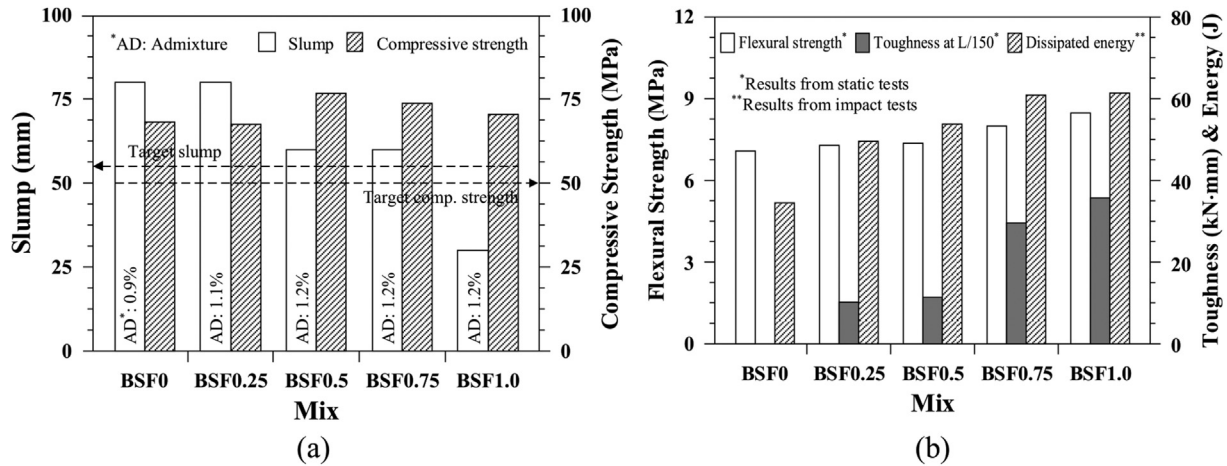


Fig. 3. Effects of fiber contents on the performance of slag concrete: (a) slump and compressive strength; (b) flexural strength, toughness and dissipated energy.

excess of the target value of 50 MPa.

The flexural strengths and toughness at a deflection of  $L/150$  obtained from static flexural tests as well as the dissipated energy measured from the impact tests are presented in Fig. 3(b). The steel fiber-reinforced slag concretes exhibited a 3–20% increase in flexural strength compared to concrete without steel fibers, and the flexural strength increased with increasing amounts of steel fiber up to a volume fraction of 1.0%. The toughness also increased with increasing volume fraction of steel fibers. The toughness gain of concrete with 0.5, 0.75, and 1.0% of steel fibers were 11, 190, and 250%, respectively, compared to the concrete with 0.25% of steel fibers. This improvement is more significant for increased steel fiber volume fraction from 0.5 to 0.75% than for that from 0.25 to 0.5% and 0.75–1.0%. The dissipated energy, which is defined as the area under the load-displacement curves, obtained from the impact test are compared in Fig. 3(b). The results showed a similar trend to the flexural strength results up to a steel fiber ratio of 0.75%, that is, the higher dissipated energy was obtained from the specimens with higher amount of steel fibers. However, further improvement was not observed for increased steel fiber volumes from 0.75 to 1.0%.

By considering all of the factors discussed in this section, concrete with fiber contents of 0.75 and 1.0% showed improved performance in terms of flexural strength and toughness under static flexure as well as the dissipated energy under impact loading compared to other concretes. The mix with 1% of steel fibers exhibited a significant decrease in workability, therefore, a 0.75% steel fiber content was chosen as the slag concrete mix for eco-friendly prestressed concrete sleeper application. It is obvious that this mix is also more economical compared to the mix with 1.0% of steel fibers.

### 3. Prototype sleeper production and test setup for the performance evaluation

#### 3.1. Prototype sleeper production

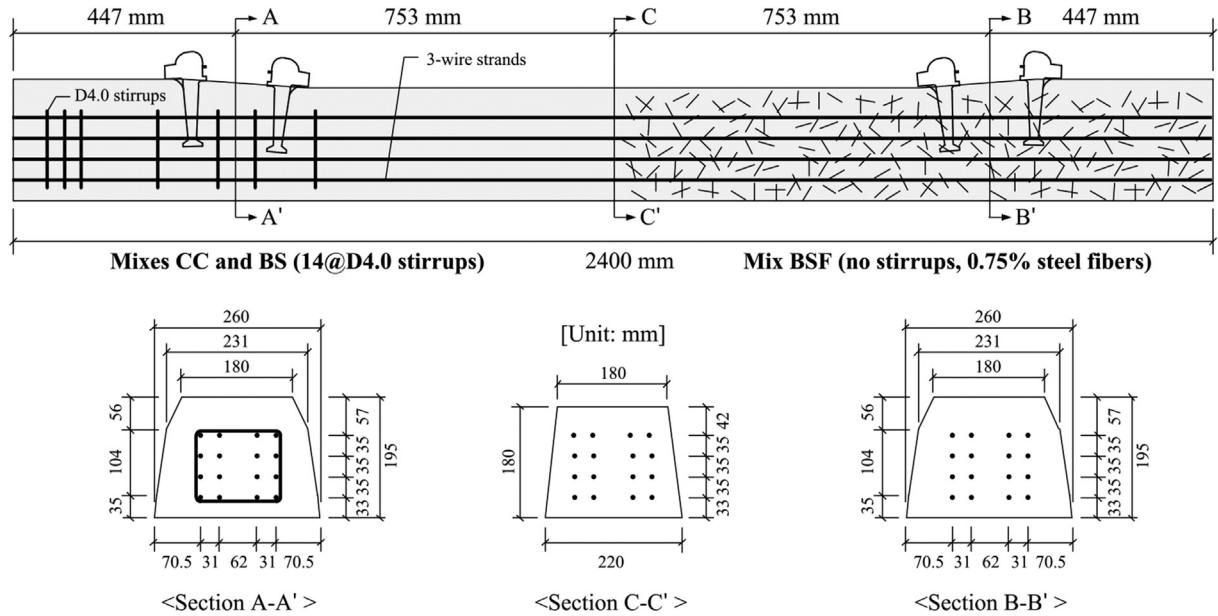
The appropriate mix proportions for the prestressed concrete sleepers, which was decided using a 56% replacement ratio of GGBFS (BS56), showed sufficient workability, early-age strength, and lower CO<sub>2</sub> emissions. The mix with 56% GGBFS and 0.75% steel fibers (BSF0.75) meets the workability and strength requirements as well as showed enhanced flexural performance. Therefore, the BS56 and BSF0.75 (BS56 + 0.75% steel fiber) mixes were chosen for

general eco-friendly railway sleeper applications and high-performance eco-friendly railway sleeper applications, respectively. For ease of reference the chosen mixes BS56 and BSF0.75 are referred to as mix BS, and mix BSF, respectively. Although these mixes have been developed by the organized mix design process described in Section 2 and the properties of the mixes were demonstrated by a series of laboratory tests, pilot production of prototype sleepers and evaluation of their mechanical properties are necessary to assure quality control of concrete under factory mass production. Furthermore, because railway sleepers are exposed to severe environmental conditions during service, it is necessary that prestressed concrete sleepers with new concrete mixes provide sufficient durability performance.

A total of ninety prestressed concrete sleepers were fabricated in a factory to verify the applicability of concrete mixes with GGBFS and steel fibers for railway sleeper production: 1) 32 sleepers with mix BS (four batches), 2) 32 sleepers with mix BSF (four batches), and 3) 26 sleepers with mix CC (four batches) which represents the control conventional concrete mix used for current railway sleepers. These sleepers were fabricated with the same equipment, manufacturing process, curing method, and materials, with only the concrete mixes being varied. The geometry of the sleepers and the typical stages of production of the prestressed concrete sleepers are shown in Fig. 4.

#### 3.2. Test setup and procedure: mechanical properties tests

Slump tests on random batches of concrete produced from the batch plant (1 m<sup>3</sup>/batch), were carried out during the fabrication of the ninety sleepers. Six 100-mm-diameter by 200-mm-long cylinders were cast for every batch (four batches for each of mixes CC, BS, and BSF) from the same concrete used to produce railway sleepers. Three of those specimens were cured under the same conditions (steam curing) as the railway sleepers to simulate the sleeper concrete properties as accurately as possible, whereas the other three cylinders were moist cured to determine if the specified compressive strength was attained. The compressive strengths at 16 h and 28 days were obtained from the same tests method described in Section 2.1.4. Each of two prismatic specimens for every batch, with dimensions of 100 × 100 × 400 mm, was cast and tested under third-point loading to determine the flexural strength. The same test method described in Section 2.2.2 was applied.



(a)



(b)

Fig. 4. Prestressed concrete sleeper production: (a) geometry of sleepers; (b) sleeper production (pretensioned strands, concrete casting, and after steam curing).

3.3. Test setup and procedure: durability tests

3.3.1. Chloride migration test (chloride permeability test)

The chloride migration test according to NT BUILD 492 [35] (known as the non-steady-state migration test) was carried out after 28 days of moist curing to investigate the chloride ion penetration resistance. This test method is capable of addressing the criticisms of the “rapid chloride permeability test” of ASTM C1202 [36] related to examination of actual chloride ion movement and temperature rise [37]. Cylindrical specimens with a diameter of 100 mm and a thickness of 50 mm, sliced from the randomly selected cast cylinders ( $\phi 100 \times 200$  mm) for each variable, were installed in cells that are able to produce a voltage difference between the positive pole in the anolyte solution of 0.3 M NaOH and the negative pole in the catholyte solution of 10% NaCl (see Fig. 5). Test voltage and duration were determined based on the initial current,  $I_{30V}$ , corresponding to the preset voltage of 30 V. The temperature of the solution was maintained at  $23 \pm 1.0$  °C and the final current after the testing was recorded. In order to measure the

chloride penetration depth after the migrations test, the specimens were split into two pieces and a 0.1 M silver nitrate solution ( $AgNO_3$ ) was sprayed on to the freshly split section. The chloride penetration depth can be measured when the white silver chloride precipitation on the split surface is clearly visible. An average of the sixteen measurements was used to determine the depth of the chloride penetration.

3.3.2. Accelerated carbonation test

The accelerated carbonation test was performed in accordance with KS F2584 [38] to investigate carbonation resistance. Carbonation of concrete reduces the natural alkalinity of the concrete, resulting in a reduction of concrete mechanical properties as well as the corrosion of strands in the railway sleepers [20,39]. The prismatic beam specimens ( $100 \times 100 \times 400$  mm) were cast and cured in moisture storage for four weeks, followed by another four weeks of curing in air at ambient temperature and at a relative humidity of 60%. The top and bottom surfaces and both end faces of the specimens, which were randomly selected from the cast beams,

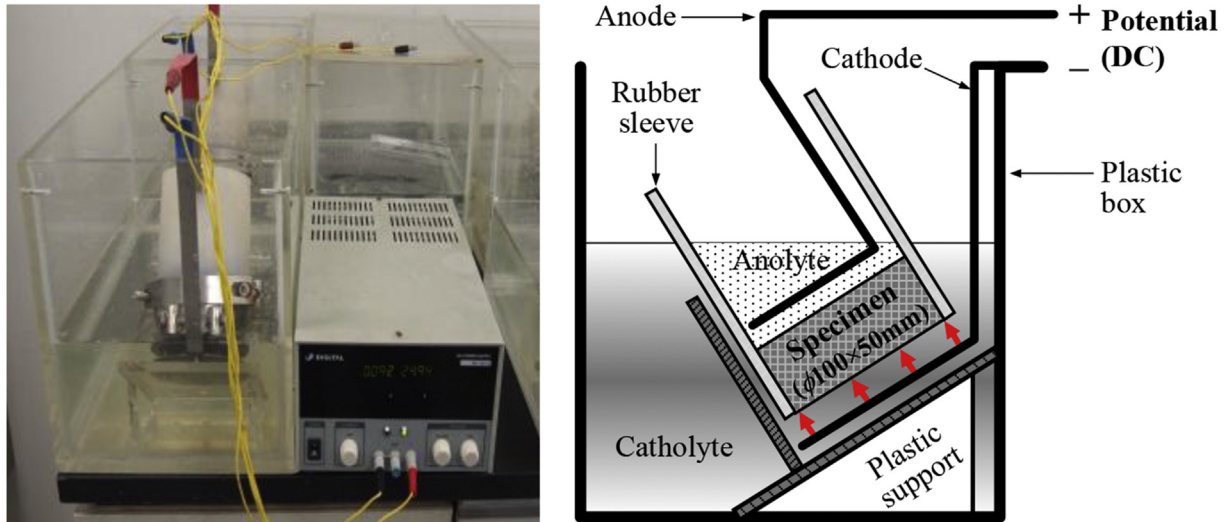


Fig. 5. Chloride migration test (chloride permeability test) setup.

were coated using polyurethane (see Fig. 6(a)) and the specimens were vertically positioned in the chamber (see Fig. 6(b)). This test setup results in only two side surfaces uniformly exposed to the carbon dioxide ( $\text{CO}_2$ ) and one-dimensional penetration of  $\text{CO}_2$  was assured. Initially the specimens were placed in the accelerated carbonation chamber for 24 h without  $\text{CO}_2$  and then the specimens were exposed to the carbonation environment for eight weeks. The accelerated carbonation chamber strictly maintains the  $\text{CO}_2$  concentration of  $5 \pm 0.2\%$ , relative humidity of  $60 \pm 5\%$ , and temperature of  $20 \pm 2\%$  for eight weeks of testing. The specimens were removed from the chamber every two weeks during the eight weeks of testing and each 60 mm-thick sample was cut (see Fig. 6(a) and (c)). In order to measure the carbonation depth, a 1% phenolphthalein solution was sprayed on a cut surface of the sample and the carbonation depth was measured from a total ten points on each sample (see Fig. 6(a)).

### 3.3.3. Rapid freezing and thawing resistance test and scaling resistance test

Repeated freezing and thawing causes cover spalling, surface scaling, and internal cracking of the concrete. Even worse, Zi et al.

[40] found that freezing of the water leaking into the sleeper can cause localized cone-shaped failures on the surfaces of the railway sleepers. It is essential that prestressed concrete sleepers have adequate resistance to repeated freeze-thaw cycles.

Two prismatic beam specimens ( $100 \times 100 \times 400$  mm) for each concrete mix were randomly selected from beams cast from every batch and they were tested under repeated freezing ( $4$  to  $-18$  °C) and thawing ( $-18$  to  $4$  °C) cycles in accordance with KS F2584 [41] which is equivalent to ASTM C666 [42]. The fundamental transverse frequency, to determine the relative dynamic modulus of elasticity, and the mass of each specimen were measured at every 30 freeze-thaw cycles, somewhat less than the recommended duration of 36 cycles.

The surface deterioration was also observed at the same cycles along with the measurement of mass changes in compliance with the visual rating suggested by ASTM C672 [43]. It is noted that ASTM C672 was originally designed to evaluate the scaling resistance of concrete surfaces exposed to freeze-thaw cycles in the presence of deicing chemicals. Although this study was conducted under freeze-thaw cycles without deicing chemicals, this observation provides some insight into the scaling resistance of concrete. Adapting those two methods, the visual rating of surface deterioration and the measurement of mass changes, increased the reliability of the data collected.

## 4. Performance of concrete for railway sleepers and discussions

### 4.1. Mechanical properties test results

The mechanical properties of the concrete for the railway sleepers, which were obtained from the tests on concrete for the pilot production, are presented in Table 6 and compared to the results from the laboratory tests described in Section 2. All concrete mixes exhibited at least 75 mm slump, which is similar or slightly higher than the results from laboratory tests, therefore, they had sufficient workability for casting and satisfied the target slump. It is noted that 1.0–1.2% of water reducing admixture was used during the ninety sleeper production. The compressive strengths determined immediately after steam curing (at 16 h after casting) ranged from 37.7 to 44.9 MPa, which exceeds the strength requirement for strand release as required in KRS TR 0008 [21]. It is noted that this

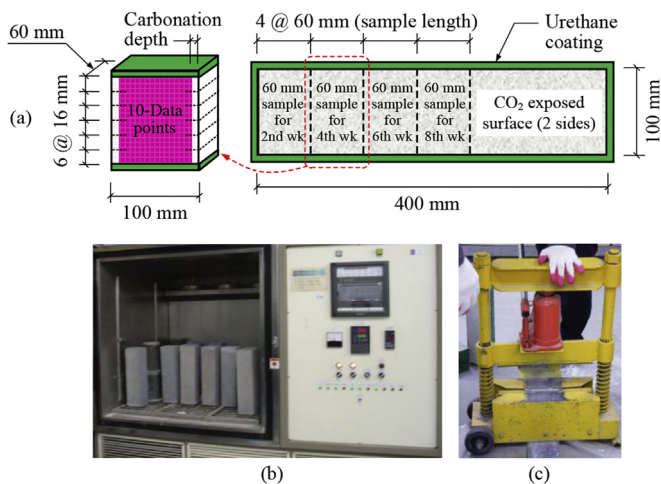


Fig. 6. Accelerated carbonation testing: (a) test specimen (b) accelerated carbonation chamber; (c) specimen cutting.



**Table 6**  
Mechanical properties of concrete for railway sleepers.

| Mix             | Slump [mm] |                 |                  | Compressive strength [MPa]     |                          |                  |                                  |                          |                  | Flexural strength [MPa] |             |                  |
|-----------------|------------|-----------------|------------------|--------------------------------|--------------------------|------------------|----------------------------------|--------------------------|------------------|-------------------------|-------------|------------------|
|                 | (>60 mm)   |                 |                  | At 16 h <sup>c</sup> (>35 MPa) |                          |                  | At 28 day <sup>d</sup> (>50 MPa) |                          |                  | At 28 day               |             |                  |
|                 | Plant      | Lab.            | P/L <sup>b</sup> | Plant                          | Lab.                     | P/L <sup>b</sup> | Plant                            | Lab.                     | P/L <sup>b</sup> | Plant                   | Lab.        | P/L <sup>b</sup> |
| CC              | 75         | 75              | 1.00             | 37.7 (0.60)                    | 54.2 (1.58)              | 0.70             | 60.5 (2.86)                      | 72.1 (4.79)              | 0.84             | 5.25 (0.74)             | 5.87 (1.11) | 0.89             |
| BS <sup>a</sup> | 80         | 80 <sup>a</sup> | 1.00             | 41.5 (0.46)                    | 51.8 <sup>a</sup> (1.20) | 0.79             | 52.5 (1.06)                      | 69.5 <sup>a</sup> (6.93) | 0.75             | 6.88 (0.30)             | 7.08 (0.47) | 0.97             |
| BSF             | 75         | 60              | 1.25             | 44.9 (1.12)                    | –                        | –                | 57.9 (0.87)                      | 73.8 (5.19)              | 0.78             | 7.36 (0.56)             | 7.99 (0.59) | 0.92             |

Items in parentheses ( ) = standard deviation.

<sup>a</sup> The average values of mix BS56 in Table 3 and mix BSF0 in Fig. 3.

<sup>b</sup> The ratio of the results from the plant pilot tests (“Plant”) to the results from laboratory tests (“Lab.”).

<sup>c</sup> Testing has been performed after steam curing.

<sup>d</sup> Testing has been performed after moisture curing.

strength requirement in the 2015 version of KRS TR 0008 has been relaxed to 30 MPa from 35 MPa [21,44]. The mixes with GGBFS (mixes BS and BSF) showed the development of higher early-age strengths than the control mix with Type III Cement (mix CC), resulting in advantages in terms of earlier strand release and form stripping. All mixes also developed strengths well above that of the specified target compressive strength at 28 days. These results demonstrate the reliability of concrete mixes developed in this study and these mixes can be used to produce eco-friendly railway sleepers under the same production process for conventional sleepers. Although the prestressed concrete sleepers are precast members and quality control is easier than in the field, the compressive strengths of the concrete from the batch plant were significantly lower than those from the laboratory trial batches at both 16 h (21–30% lower) and 28 days (16–25% lower). The flexural strengths also showed similar trends with the values obtained from the batch plant being 3–11% lower than those from the laboratory trial batches. These results demonstrate the importance of adequate quality control of the concrete in the production of prestressed concrete sleepers. ACI Committee for high-strength concrete (ACI 363R-10) [45] also reported the fact that “laboratory trial batches frequently exhibit significantly higher strength than can be reasonably achieved in production”. According to this committee, possible reasons for this difference can be attributed to variations in temperatures, dust around aggregates stored in yards, moisture conditions of the aggregates and the efficiency of the plant concrete mixer.

#### 4.2. Durability test results

##### 4.2.1. Chloride migration test results

The chloride penetration depths and the chloride ion diffusion coefficients (also known as the non-steady-state chloride migration coefficient) for three different mixes are presented in Fig. 7. Both parameters are used to quantify the concrete resistance to chloride penetration. The chloride ion diffusion coefficient is calculated on the basis of the voltage magnitude, temperature of anolyte measured at the beginning and end of test and the depth of penetration of the chloride ions, using the following equations [35,46,47]:

$$D_{cpd} = \frac{RT}{zFE} \cdot \frac{x_d - \alpha\sqrt{x_d}}{t} \quad (2)$$

where,  $E = \frac{U-2}{L}$  and  $\alpha = 2\sqrt{\frac{RT}{zFE}} \cdot \text{erf}^{-1} \left( 1 - \frac{2c_d}{c_0} \right)$ ,  $D_{cpd}$ : chloride ion diffusion coefficient (m<sup>2</sup>/sec),  $z$ : absolute value of ion valence (for chloride ions,  $z = 1$ ),  $F$ : Faraday constant ( $9.6481 \times 10^4$  J/V·mol),  $U$ : absolute value of the applied voltage (V),  $R$ : gas constant (8.314 J/K·mol),  $T$ : average value of the initial and final temperatures in the anolyte solution (K),  $L$ : thickness of the

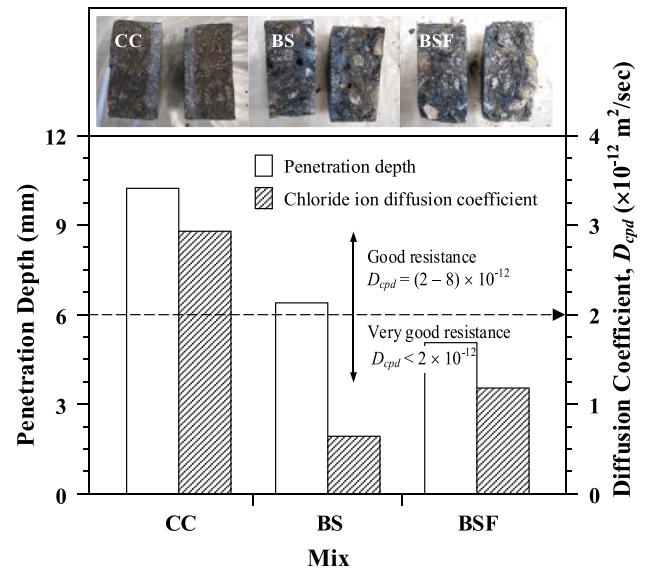


Fig. 7. Chloride ion penetration depth and diffusion coefficient results.

specimen (m),  $x_d$ : average value of the penetration depths (m),  $t$ : test duration (sec),  $\text{erf}^{-1}$ : inverse of error function,  $c_d$ : chloride ion concentration where a color is changed with nitrate ions (mol/l),  $c_0$ : chloride ion concentration the catholyte solution (mol/l).

Mixes BS and BSF exhibited 78% and 60% decreases in the diffusion coefficient (38% and 51% decreases in the penetration depth), respectively, compared to control mix CC that indicates an increased resistance to the chloride ion penetration. This result explains that GGBFS densify the concrete matrix and lowers the continuity of the pore structures, leading to a reduction of chloride ion penetration [11,13,39]. Furthermore, these results also support the fact that partial substitution of cement with GGBFS increases the chloride binding, which reduces the apparent diffusion coefficients [46–49]. It is noted that GGBFS form additional calcium aluminate hydrates (C<sub>3</sub>A and C<sub>4</sub>AF) which chemically react with a portion of the chloride ions entering the concrete, producing physically bound chlorides known as Friedel’s salt [46,49]. These physically bound chlorides hinder the movement of the remaining free chlorides through the concrete, thereby reducing the diffusion rate [37,46,49].

Tang [50] proposed limits of diffusion coefficient for evaluating the concrete resistance to chloride penetration: 1) very good resistance when  $D_{cpd} < 2 \times 10^{-12}$ ; 2) good resistance when  $2 \times 10^{-12} < D_{cpd} < 8 \times 10^{-12}$ ; 3) acceptable resistance when  $8 \times 10^{-12} < D_{cpd} < 16 \times 10^{-12}$ ; and 4) unacceptable when  $D_{cpd} > 16 \times 10^{-12}$ . Based on these criteria, the resistances of both

mixes BS and BSF to chloride ion penetration are classified as “very good”, whereas the resistance of mix CC is classified as “good”.

Within the same slag based mix, the chloride ion diffusion coefficient of mix BSF was higher than that of mix BS (diffusion coefficient increased with an increase in fiber content), resulting in a different trend compared to the results of the penetration depth (penetration depth decreased with an increase in fiber content), as shown in Fig. 7. Stanish et al. [37] and Berrocal et al. [51] reported criticism of this non-steady-state migration test (NT BUILD 492 method) when the concrete includes conductive materials. Stanish et al. [37] indicated that inclusion of conductive materials, such as metal or carbon (steel fiber in this test series), could short-circuit the migration cell, and the current is then carried by the conductor rather than the ions in the pore solution. If the conductor does not short-circuit the cell (i.e. if a piece of steel is parallel to the surface), there is the possibility of it reacting with the chloride ions and affecting ion movement in that manner. Berrocal et al. [51] indicated that if conductive fibers are added to concrete, these could influence the initial current and consequently the test parameters (i.e., the voltage applied and the duration of the test since these are based on the initial measurements of the electric current). Although both parameters are considered in the equation used to calculate the migration coefficient, this may still potentially skew the results from migration tests. Test results of Berrocal [52] showed higher diffusion coefficients in steel fiber-reinforced concrete (SFRC) than plain concrete (12% increases). Abrycki and Zajdzinski [53] reported higher diffusion coefficients (average value at 35 days) in SFRC than in plain concrete for steel fiber volume fractions  $v_f = 0.3, 0.6,$  and  $1.3\%$  but the opposite result was obtained in case of  $v_f = 1.0\%$ . From a critical review of the results of the chloride diffusion coefficients of concrete with and without steel fibers from six series of literature, which was studied by Berrocal et al. [51], the ratio of diffusion coefficient of SFRC to plain concrete, ( $D_{SFRC}/D_{plain}$ ), varied approximately from 0.37 to 1.53. Therefore, further experimental research to investigate the effects of steel fibers on the diffusion coefficient of concrete is recommended, including the variables of fiber volume fractions, type, length, and orientation as well as concrete mixtures.

#### 4.2.2. Accelerated concrete carbonation test results

Fig. 8 illustrates the increase of carbonation depth in two-week intervals and Fig. 9 shows the measured carbonation depth and fractional carbonation depth versus time of exposure relationships for all the mixes. The average carbonation coefficient,  $C$  (mm/ $\sqrt{\text{day}}$ ), was also calculated using the following equation and the results are presented in Fig. 9 [54,55].

$$x = x_0 + C \cdot \sqrt{t} \quad (3)$$

where,  $x$ : the depth of carbonation (mm),  $t$ : exposure time (day), and  $x_0$ : initial carbonation (usually small or zero). The extension of carbonation depth for mix CC was difficult to ascertain visually and the carbonation coefficient was close to zero. Whereas, mixes BS and BSF exhibited a significant increase in the carbonation rate, which means that the concrete with GGBFS replaced binders is more vulnerable to carbonation than concrete with 100% Type III Portland cement. When  $\text{CO}_2$  from the air reacts with the cement paste, initially the calcium hydroxide ( $\text{Ca}(\text{OH})_2$ ) carbonates to calcium carbonate ( $\text{CaCO}_3$ ) and then calcium-silicate-hydrates (C-S-H) break down into  $\text{CaCO}_3$  and silica gel, resulting in a drop in pH [56]. Partial replacement of cement by slag results in less  $\text{Ca}(\text{OH})_2$  due to the reduction of the cement content and further reduction of  $\text{Ca}(\text{OH})_2$  occurs due to the consumption by the secondary hydration reaction with  $\text{SiO}_2$  in the slag. Therefore, the pH level of the slag concrete is already low because of the lower cement content and it

is further reduced by the chemical reaction with the slag, resulting in a decrease of carbonation resistance [56]. This result agrees well with the findings of Gruyaert et al. [54], who studied the relationship between carbonation depth and slag replacement level. Their mixture (W/B = 0.5 and unit cement weight =  $350 \text{ kg/m}^3$ ) with ordinary Portland cement exhibited no carbonation, but the carbonation depths and carbonation coefficients increased with increasing blast furnace slag content. They addressed the rapid carbonation of slag concrete in terms of low pH of pore solutions of concrete containing blast furnace slag and the preferential reaction of  $\text{CO}_2$  with  $\text{Ca}(\text{OH})_2$ . They also mentioned a more porous structure allowing  $\text{CO}_2$  to penetrate more easily in the concrete owing to increased gas permeability of the concrete with increasing slag content [54].

A comparison of the result of mixes BS and BSF indicates the beneficial effects of steel fibers on the carbonation resistance of concrete. Mix BSF with 0.75% of steel fibers showed an 18% decrease in the carbonation coefficient compared to mix BS without steel fibers. This observation coincides with the findings of Wang et al. [57]. They performed a micro-pore structure analysis and explained this phenomenon by better micro-crack control due to the steel fibers, resulting in a more compact internal structure and reduced carbon dioxide penetration. However, they also pointed out the importance of an appropriate amount of steel fibers for better carbonation resistance. They found that the carbonation depth decreases with increasing steel fiber volume fraction up to 1.5%, but carbonation depth increases when the steel fibers content is increased to 2% due to the less uniform distribution of the steel fibers.

The carbonation process affects the long-term behavior of concrete. Carbonation models for predicting the service life of concrete are presented in Fig. 9. Two types of models based on chemical reaction-controlled as predicted using Equation (4) (solid lines in Fig. 9) and diffusion-controlled as predicted by Equation (5) (dotted lines in Fig. 9), were considered [39,58].

$$\frac{t}{\tau} = 1 - (1 - X_s)^{1/2} \quad (4)$$

$$\frac{t}{\tau} = X_s + (1 - X_s) \ln(1 - X_s) \quad (5)$$

where,  $X_s$ : fractional carbonation at time  $t$ ,  $t$ : time of experiment, and  $\tau$ : time for complete carbonation. One-dimensional carbonation was assumed by coating the specimens (see Fig. 6), therefore,  $X_s$  could be easily calculated. The diffusion control model fits the test data of mix BS well and it also gives a reasonable prediction for mix BSF. However, the chemical reaction control models give poor predictions for all mixes. The reliability of the models for mix CC cannot be guaranteed because the carbonation of mix CC was almost zero. It is concluded that the carbonation of concrete mixes used in this study is governed by the diffusion controlled model, therefore, it can be used to predict the long-term carbonation resistance of the mixes.

The average carbonation coefficient, defined in Eq. (3), can be also used to predict the carbonation depth for the service life of railway sleepers. The target service life of prestressed concrete sleepers is approximately 30 years, with a range of 20–50 years [2,4,5,59]. The carbonation coefficients are based on accelerated carbonation tests, conducted at a concentration of 5.0%  $\text{CO}_2$  in this study, whereas the real  $\text{CO}_2$  concentration of air ranges between 0.03% and 0.3% [54]. Equation (6) gives the relationship for carbonation coefficients as a function of the concentration levels of  $\text{CO}_2$ .

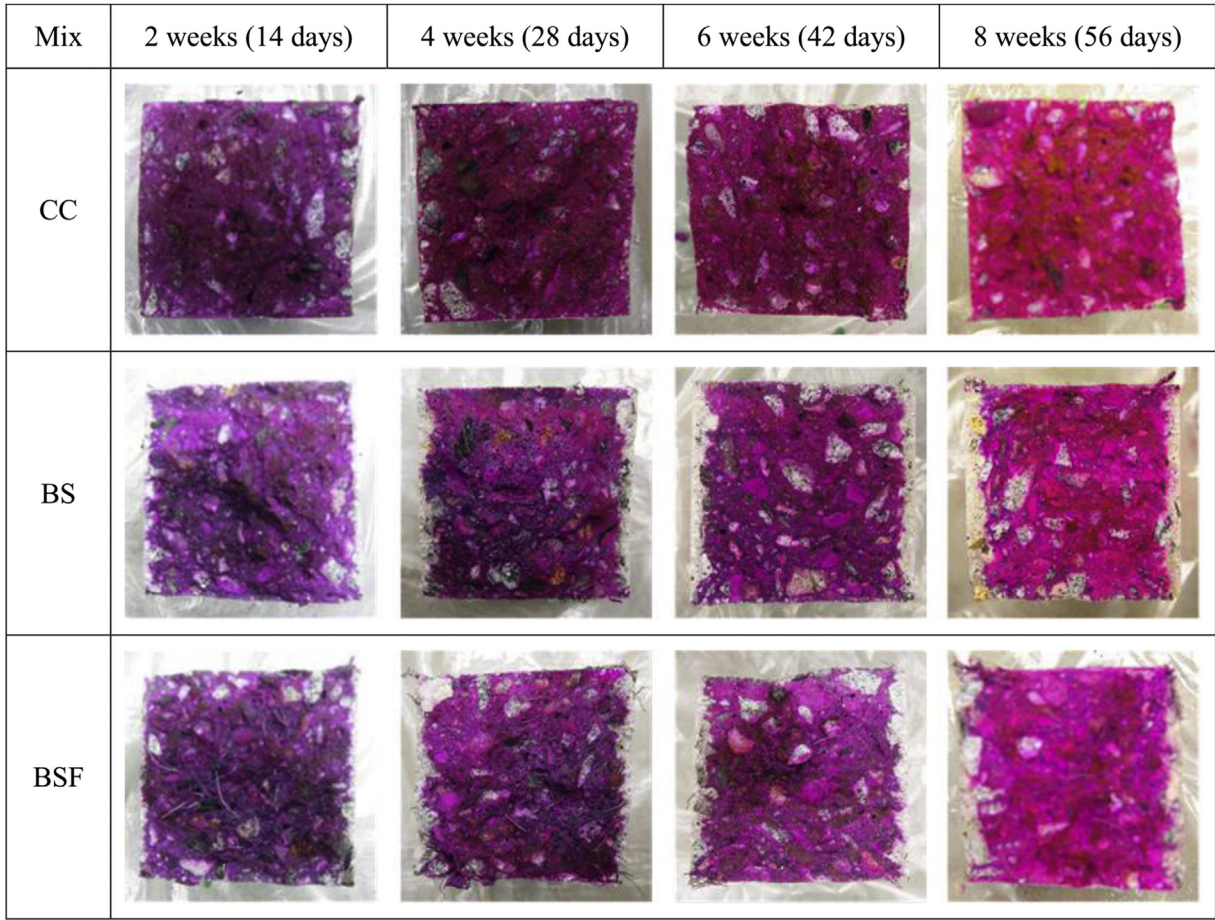


Fig. 8. Increase of carbonation depth with time.

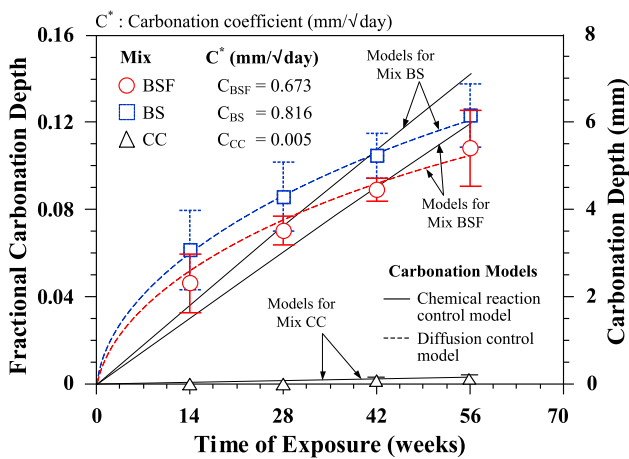


Fig. 9. Accelerated carbonation test results.

$$\frac{C_{acc}}{C_{air}} = \sqrt{\frac{(CO_2)_{acc}}{(CO_2)_{air}}} \quad (6)$$

where,  $C_{acc}$  and  $C_{air}$ : average carbonation coefficients of accelerated tests and ambient air, respectively, and  $(CO_2)_{acc}$  and  $(CO_2)_{air}$ :  $CO_2$  concentration in accelerated tests and ambient air, respectively. The concentration of  $(CO_2)_{air}$  of 0.3% and 50 years of service life were

conservatively used to calculate the depth of carbonation for mixes BS and BSF, resulting in approximately 27 and 22 mm of carbonation depth, respectively. It is noted that the other environmental conditions (i.e., curing age, actual temperature and humidity on site) affecting the carbonation coefficient in ambient air,  $C_{air}$ , were assumed to be the same as those used in the carbonation tests (given in Section 3.3.2). The concrete clear cover for the stirrups and for bottom strands are 27.55 and 31.55 mm, respectively, which are larger than the predicted depth of carbonation after 50 years. This result indicates that although carbonation of mixes with GGBFS is more rapid than with conventional concrete mixes with Type III Portland cement, eco-friendly mixes developed in this study (mixes BS and BSF) can resist carbonation for 50 years of service life.

#### 4.2.3. Rapid freezing and thawing resistance test results

The effect of freezing and thawing cycles (up to 300 cycles) on the relative dynamic modulus of elasticity is presented in Fig. 10(a). Mixes BS and BSF exhibited quite gradual decreases of up to 20 and 12% in the relative dynamic modulus of elasticity, respectively. Mix CC exhibited a sudden decrease of the relative dynamic modulus of elasticity of more than 50% between 120 and 210 cycles, and it decreased to 40% at 300 cycles. This result coincides with the results from Seo et al. [60] that showed the relative dynamic modulus of elasticity for the 30% and 60% replacement of cement by slag was higher than that of plain concrete. The 70% slag content concrete in the test from Nakamoto et al. [61] also showed slightly higher relative dynamic modulus of elasticity than slag free concrete but the 85% and 95% slag concretes showed decreased values than the

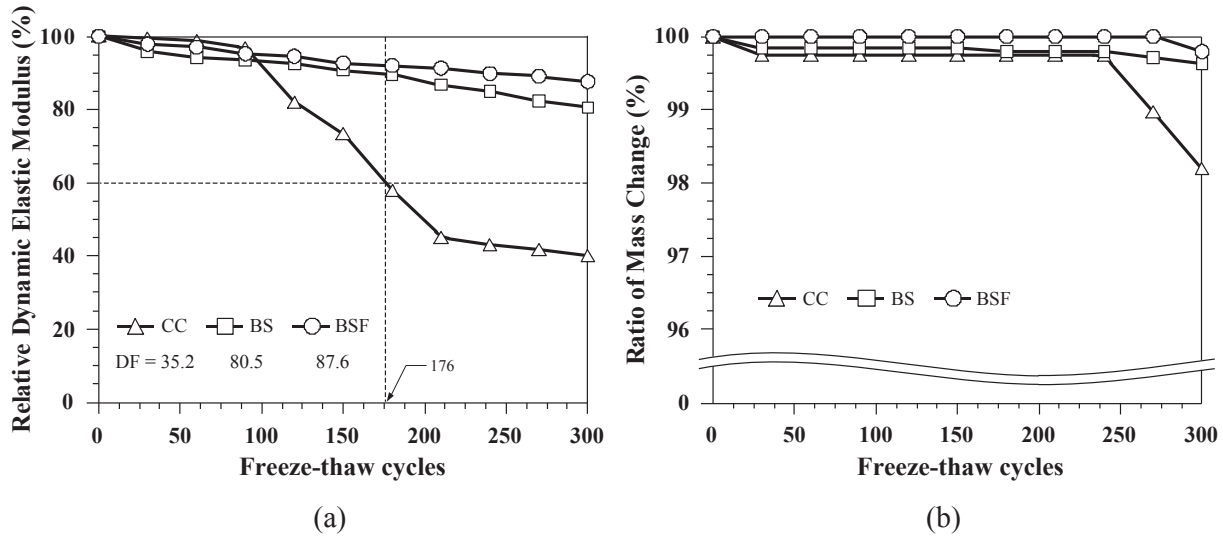


Fig. 10. Freezing and thawing resistance results: (a) relative dynamic modulus of elasticity (%); (b) ratio of mass change (%).

slag free concrete. Hooton [56] and ACI Committee 233 [62] who reviewed the effects of GGBFS on the performance of concrete reported that there is no detrimental effect of slag on freeze and thaw resistance of the concrete.

The durability factor,  $DF$ , is used to evaluate the freezing and thawing resistance of concrete:

$$DF = \frac{P \times N}{M} \quad (7)$$

where  $P$ : relative dynamic modulus of elasticity at  $N$  cycles (%),  $N$ : number of cycles at which  $P$  reaches the specified minimum value (60%) for discontinuing the test or the specified number of cycles at which the exposure is to be terminated, whichever is less, and  $M$ : specified number of cycles at which the exposure is to be terminated (300 cycles). In general, concrete is judged to be resistant to freezing and thawing when  $DF$  is larger than 60 [63]. The relative dynamic modulus of elasticity of mix CC was lower than 60% after 176 cycles, resulting in a  $DF$  of 35.2. Therefore, the conventional concrete mix for prestressed concrete sleepers with type III cement may deteriorate by the freezing and thawing action of concrete. In contrast, mixes containing GGBFS only and GGBFS with steel fibers (mixes BS and BSF) may have sufficient resistance to deterioration from freeze-thaw cycles. Thus, concrete including GGBFS is more suitable for the production of railway sleepers that are situated in climates having a large number of freeze-thaw cycles.

The surface deterioration of concrete was examined by the ratio of mass change (see Fig. 10(b)) as well as the visual rating method (see Fig. 11). The surface observation was performed at the same number of cycles along with the measurement of mass change (every 30 cycles). Photographs for three typical cycles (0, 150, and 300 cycles) are shown in Fig. 11. Mixes BS and BSF exhibited less than 0.36% mass loss over the 300 cycles of freezing and thawing. The ratio of mass change of mix CC was quite similar to mix BS up to 240 cycles, but it exhibited a relatively sudden decrease compared to mixes BS and BSF after 240 cycles. The results from the surface observations visually confirmed the mass changes of the concrete. These results demonstrate that mix CC started to deteriorate not only in the interior matrix, but also on the surface because of the repeated volume change of the water in the pores. Mix BSF with 0.75% steel fibers had a slightly better freezing and thawing resistance than mix BS, in terms of relative dynamic modulus of

elasticity, ratio of mass change, and surface scaling. In summary, the partial replacement of cement with GGBFS can significantly improve the freeze-thaw resistance compared to that of Portland cement concrete, and further improvement can be achieved by adding steel fibers ( $v_f = 0.75\%$ ) to the mixes. Therefore, prestressed concrete sleepers produced with these mixes are expected to have a longer service life.

## 5. Conclusions

The use of ground granulated blast furnace slag (GGBFS) and steel fibers for concrete mixes for railway sleepers has been investigated. The appropriate mix proportions, mechanical properties, and durability performance of these mixes were discussed in this study, and following conclusions can be drawn:

- 1) The mix proportions with partial replacement of Type III Portland cement by ground granulated blast furnace slag were evaluated and mixes with a 56% slag replacement level showed not only improved performance but also less CO<sub>2</sub> emissions.
- 2) The use of 0.75% of steel fibers in a slag concrete mix results in enhanced static and impact flexural capacity and toughness as well as sufficient workability for concrete casting.
- 3) Using new mixes incorporating GGBFS and GGBFS with steel fibers, a total of ninety prestressed concrete sleepers were produced under the same production process used for conventional railway sleepers. Concrete with the new mixes exceeded the strength requirements of the Korean Railway Standard but the strengths were somewhat lower than the laboratory mix test results. This underlines the need for careful quality control of the concrete for producing prestressed concrete sleepers.
- 4) The durability performance of the concrete mixes for prestressed concrete sleepers was also evaluated in terms of chloride ion penetration, carbonation, freezing and thawing, and scaling resistance. The mix with GGBFS (partial replacement of Type III Portland cement by GGBFS) showed improved resistance to chloride ion penetration and freeze-thaw cycles compared to the conventional concrete mix currently used for railway sleepers. The mix with GGBFS was more vulnerable to carbonation, however the predicted depth of carbonation was less than the concrete cover after 50 years of service.


















| Cycle     | Mix CC  |   | Mix BS  |  | Mix BSF   |   |
|-----------|---|---|---|--|---|---|
|           | Specimen 1  | Specimen 2  | Specimen 1  | Specimen 2   | Specimen 1  | Specimen 2  |
| 0 cycle   |    |    |    |    |    |    |
| 150 cycle |   |   |   |   |   |   |
| 300 cycle |  |  |  |  |  |  |

Fig. 11. Concrete surface scaling at different freeze-thaw cycles.

- 5) The mix with GGBFS and steel fibers (mix BSF) showed a slightly better durability performance than the mix with GGBFS only (mix BS), including better carbonation and freeze-thaw resistances. The mix BSF showed decreased chloride ion penetration depth than mix BS, but showed a slightly higher chloride ion diffusion coefficient.

### Acknowledgements

This work was supported by the Industrial Strategic technology development program (10063488, Development of Earthquake Resisting Reinforced Concrete using grade 700 MPa Reinforcing Bars for enhancement of seismic safety) funded by the Ministry of Trade, Industry and Energy and Basic Science Research Program through the National Research Foundation of Korea (NRF) funded by the Ministry of Education, Science and Technology (NRF-2014R1A6A3A03056173).

### Notation

|            |   |
|------------|---|
| $C_e$      | total CO <sub>2</sub> emission  |
| $CO_{2-M}$ | CO <sub>2</sub> emissions from the raw material phases  |
| $CO_{2-T}$ | CO <sub>2</sub> emissions from the transportation phases  |
| $CO_{2-P}$ | CO <sub>2</sub> emissions from the concrete production phases                                       |
| $v_f$      | steel fiber volume fraction   |
| $l/d$      | aspect-ratio of steel fiber   |
| $D_{cpd}$  | chloride diffusion coefficient or non-steady-state migration coefficient (m <sup>2</sup> /sec)      |
| $F$        | Faraday constant ( $9.6481 \times 10^4$ J/V·mol)  |
| $U$        | absolute value of the applied voltage (V)   |
| $R$        | gas constant (8.314 J/K·mol)  |
| $T$        | average value of the initial and final temperatures in the anolyte solution (K)                     |
| $L$        | thickness of the specimen (m)   |
| $x_d$      | average value of the penetration depths (m)   |
| $erf^{-1}$ | inverse of error function   |
| $c_d$      | chloride ion concentration where a color is changed with nitrate ions (mol/l)                       |
| $c_o$      | chloride ion concentration the catholyte solution (mol/l)   |
| $x$        | depth of carbonation (mm)   |
| $x_0$      | initial carbonation   |
| $C$        | carbonation coefficient   |
| $X_s$      | fractional carbonation at time $t$  |
| $\tau$     | time for complete carbonation   |
| $C_{acc}$  | average carbonation coefficient at accelerated tests  |
| $C_{air}$  | average carbonation coefficient at air  |
| $DF$       | durability factor   |
| $P$        | relative dynamic modulus of elasticity at $N$ cycles (%)  |
| $N$        | number of cycles at which $P$ reaches the specified minimum value or the specified number of cycles |
| $M$        | specified number of cycles at which the exposure is to be terminated                                |

### References

- [1] J. Zhao, A.H.C. Chan, M.P.N. Burrow, Reliability analysis and maintenance decision for railway sleepers using track condition information, *J. Op. Res. Soc.* 58 (2007) 1047–1055.
- [2] A. Manalo, T. Aravinthan, W. Karunasena, A. Ticoalu, A review of alternative materials for replacing existing timber sleepers, *Compos. Struct.* 92 (2010) 603–611.
- [3] J. Taherinezhad, M. Sofi, P. Mendis, T. Ngo, A review of behaviour of prestressed concrete sleepers, *Electron. J. Struct. Eng.* 13 (2013) 1–16.
- [4] W. Ferdous, A. Manalo, Failures of mainline railway sleepers and suggested remedies – review of current practice, *Eng. Fail. Anal.* 44 (2014) 17–35.
- [5] W. Ferdous, A. Manalo, G. Van Erp, T. Aravinthan, S. Kaewunruen, A. Remennikov, Composite railway sleepers – recent developments, challenges and future prospects, *Compos. Struct.* 134 (2015) 158–168.
- [6] M. Shojaei, K. Behfarnia, R. Mohebi, Application of alkali-activated slag concrete in railway sleepers, *Mater. Des.* 69 (2015) 89–95.
- [7] KEITI (Korea Environmental Industry & Technology Institute), Korea LCI Database Information Network. <http://www.edp.or.kr/lci/>.
- [8] K.H. Yang, Y.B. Jung, M.S. Cho, S.H. Tae, Effect of supplementary cementitious materials on reduction of CO<sub>2</sub> emissions from concrete, *J. Clean. Prod.* 103 (2014) 774–783.
- [9] D.M. Flower, J. Sanjayan, Green house gas emissions due to concrete manufacture, *Int. J. Life Cycle Assess.* 12 (2007) 282–288.
- [10] R.H. Lutch, D.K. Harris, T.M. Ahlborn, Prestressed concrete ties in North America, in: *Proceedings of AREMA 2009 Annual Conference*, Chicago, USA, 2009.
- [11] B.M. Mithun, M.C. Narasimhan, Performance of alkali activated slag concrete mixes incorporating copper slag as fine aggregate, *J. Clean. Prod.* 112 (2016) 837–844.
- [12] H. Yazici, M.Y. Yardimci, H. Yiğiter, S. Aydın, S. Türkel, Mechanical properties of reactive powder concrete containing high volumes of ground granulated blast furnace slag, *Cem. Concr. Compos.* 32 (2010) 639–648.
- [13] J.P. Won, H.H. Kim, S.J. Lee, S.J. Choi, Carbon reduction of precast concrete under the marine environment, *Constr. Build. Mater.* 74 (2015) 118–123.
- [14] T. Koh, S. Hwang, Field evaluation and durability analysis of an eco-friendly prestressed concrete sleeper, *J. Mater. Civ. Eng.* 27 (2015) B4014009.
- [15] ACI Committee 544, Report on Fiber Reinforced Concrete (544.1R-96), American Concrete Institute, Farmington Hills, MI, 1996.
- [16] H. Shin, Y. Yoon, S. Lee, W. Cook, D. Mitchell, Effect of steel fibers on the performance of ultrahigh-strength concrete columns, *J. Mater. Civ. Eng.* 27 (2015) 04014142.
- [17] H. Aoude, M. Belghiti, W.D. Cook, D. Mitchell, Response of steel fiber-reinforced concrete beams with and without stirrups, *ACI Struct. J.* 109 (2012) 359–368.
- [18] H. Aoude, W.D. Cook, D. Mitchell, Behavior of columns constructed with fibers and self-consolidating concrete, *ACI Struct. J.* 106 (2009) 349–357.
- [19] H.H. Dinh, Shear Behavior of Steel Fiber Reinforced Concrete Beams without Stirrup Reinforcement [Ph.D. Thesis], University of Toronto, Toronto, ON, 2009.
- [20] M.P. Collins, D. Mitchell, *Prestressed Concrete Structures*. Montreal/Toronto, Response publications, Canada, 1997, p. p.30.
- [21] KRS TR 0008–11(R), Prestressed Concrete Sleeper, Korean Railway Standards, Gyeonggi Province, South Korea, 2011.
- [22] Taemyung Industrial Co. Ltd, KNR Sleeper for 60kgK Rail (KRS TR 0008), 2008. Gyeonggi Province, South Korea.
- [23] Y. Yoon, et al., Development of Optimal Concrete Mixture for Prestressed Concrete Sleepers [Research Report], Korea University, Seoul, South Korea, 2012.
- [24] Portland Cement Association (PCA), *Ettringite Formation and the Performance of Concrete*, Portland Cement Association, Skokie, Illinois, 2001.
- [25] ASTM C143/C143M-15, Standard Test Method for Slump of Hydraulic-cement Concrete, ASTM International, West Conshohocken, PA, 2015.
- [26] ASTM C39/C39M-15a, Standard Test Method for Compressive Strength of Cylindrical Concrete Specimens, ASTM International, West Conshohocken, PA, 2015.
- [27] Ö. Eren, Strength development of concretes with ordinary Portland cement, slag or fly ash cured at different temperatures, *Mater. Struct.* 35 (2002) 536–540.
- [28] J.K. Kim, Y.H. Moon, S.H. Eo, Compressive strength development of concrete with different curing time and temperature, *Cem. Concr. Res.* 28 (1998) 1761–1773.
- [29] K.H. Yang, J.K. Song, K.I. Song, Assessment of CO<sub>2</sub> reduction of alkali-activated concrete, *J. Clean. Prod.* 39 (2013) 265–272.
- [30] ISO 14040, Environmental Management – Life Cycle Assessment – Principles and Framework, International Standard Organization, 2006.
- [31] S. Joshi, Product environmental life-cycle assessment using input-output techniques, *J. Indust. Ecol.* 3 (2000) 95–120.
- [32] D.Y. Yoo, Y.S. Yoon, N. Banthia, Flexural response of steel-fiber-reinforced concrete beams: effects of strength, fiber content, and strain-rate, *Cem. Concr. Compos.* 64 (2015) 84–92.
- [33] D.Y. Yoo, Y.S. Yoon, Influence of steel fibers and fiber-reinforced polymers on the impact resistance of one-way concrete slabs, *J. Compos. Mater.* 48 (2014) 695–706.
- [34] ASTM C1609/1606M-12, Standard Test Method for Flexural Performance of Fiber-reinforced Concrete (Using Beam with Third-point Loading), ASTM International, West Conshohocken, PA, 2012.
- [35] NT Build 492, Concrete, Mortar and Cement-based Repair Materials: Chloride Migration Coefficient from Non-steady-state Migration Experiments, 1999. Espoo, Finland. NORDTEST.
- [36] ASTM C1202-12, Standard Test Method for Electrical Indication of Concrete's Ability to Resist Chloride Ion Penetration, ASTM International, West Conshohocken, PA, 2012.
- [37] K. Stanish, R.D. Hooton, M. Thomas, Testing the Chloride Penetration Resistance of Concrete: a Literature Review [Research Report], University of Toronto, Toronto, ON, 2001.
- [38] KS F 2584, Standard Test Method for Accelerated Carbonation of Concrete, Korea Standard Association, Seoul, South Korea, 2010.
- [39] S.A. Bernal, R.M. de Gutiérrez, A.L. Pedraza, J.L. Provis, E.D. Rodriguez, S. Delvasto, Effect of binder content on the performance of alkali-activated

- slag concretes, *Cem. Concr. Res.* 41 (2011) 1–8.
- [40] G. Zi, D.Y. Moon, S.J. Lee, S.Y. Jang, S.C. Yang, S.-S. Kim, Investigation of a concrete railway sleeper failed by ice expansion, *Eng. Fail. Anal.* 26 (2012) 151–163.
- [41] KS F 2456, Standard Test Method for Resistance of Concrete to Rapid Freezing and Thawing, Korea Standard Association, Seoul, South Korea, 2013.
- [42] ASTM C666/C666M-15, Resistance of Concrete to Rapid Freezing and Thawing, ASTM International, West Conshohocken, PA, 2015.
- [43] ASTM C672/C672M-12, Standard Test Method for Scaling Resistance of Concrete Surfaces Exposed to Deicing Chemicals, ASTM International, West Conshohocken, PA, 2012.
- [44] KRS TR 0008–15(R), Prestressed Concrete Sleeper, Korean Railway Standards, Gyeonggi Province, South Korea, 2015.
- [45] ACI Committee 363, Report on High-strength Concrete (363R-10), American Concrete Institute, Farmington Hills, MI, 2010.
- [46] E. Karkar, Developing and Evaluating Rapid Test Methods for Measuring the Sulphate Penetration Resistance of Concrete in Relation to Chloride Penetration Resistance [Degree of Master of Applied Science], University of Toronto, Toronto, ON, 2011.
- [47] T. Zych, Test methods of concrete resistance to chloride ingress, *Civil Engineering Issue 6-B, Tech. Trans.* 21 (2014) 117–139.
- [48] H. Justnes, A review of chloride binding in cementitious systems, *Nordic Concr. Res. Publ.* 21 (1998) 48–63.
- [49] Q. Yuan, C. Shi, G. De Schutter, K. Audenaert, D. Deng, Chloride binding of cement-based materials subjected to external chloride environment – a review, *Constr. Build. Mater.* 23 (2009) 1–13.
- [50] L. Tang, Chloride Transport in Concrete – Measurement and Prediction [Ph.D. Thesis], Chalmers University of Technology, Gothenburg, Sweden, 1996.
- [51] C.G. Berrocal, K. Lundgren, I. Löfgren, Corrosion of steel bars embedded in fibre reinforced concrete under chloride attack: state of the art, *Cem. Concr. Res.* 80 (2016) 69–85.
- [52] C.G. Berrocal, Chloride Induced Corrosion of Steel Bars in Fibre Reinforced Concrete [Thesis for the Degree of Licentiate of Engineering], Chalmers University of Technology, Göteborg, 2015.
- [53] M. Abrycki, A. Zajdzinski, Effect of Fibres on Corrosion of Steel Reinforcement [Degree of Master of Science], Chalmers University of Technology, Göteborg, 2012.
- [54] E. Gruyaert, P. Van den Heede, N. De Belie, Carbonation of slag concrete: effect of the cement replacement level and curing on the carbonation coefficient – effect of carbonation on the pore structure, *Cem. Concr. Compos.* 35 (2013) 39–48.
- [55] P.H.R. Borges, J.O. Costa, N.B. Milestone, C.J. Lynsdale, R.E. Streatfield, Carbonation of CH and C–S–H in composite cement pastes containing high amounts of BFS, *Cem. Concr. Res.* 40 (2010) 284–292.
- [56] R.D. Hooton, Canadian use of ground granulated blast-furnace slag as a supplementary cementing material for enhanced performance of concrete, *Can. J. Civ. Eng.* 27 (2000) 754–760.
- [57] Y. Wang, D. Niu, Z. Dong, Experimental study on carbonation of steel fiber reinforced concrete, in: 4th International Conference on the Durability of Concrete Structures, Purdue University, West Lafayette, IN, 2014, pp. 55–59.
- [58] M. Castellote, C. Andrade, Modelling the carbonation of cementitious matrixes by means of the unreacted-core model, UR-CORE, *Cem. Concr. Res.* 38 (2008) 1374–1384.
- [59] R.H. Crawford, Greenhouse gas emissions embodied in reinforced concrete and timber railway sleepers, *Environ. Sci. Technol.* 43 (2009) 3885–3890.
- [60] T. Seo, Y. Jung, J. Kim, O. Na, Durability of steam-cured concrete with slag under the combined deterioration of freezing-thawing cycles and deicing chemicals, *Struct. Concr.* (2016), <http://dx.doi.org/10.1002/suco.201500201>. Accepted.
- [61] J. Nakamoto, K. Togawa, T. Miyagawa, M. Fujii, S. Nagaoka, Freezing and Thawing Resistance of High Slag Content Concrete, ACI Special Publication, 1998, pp. 1059–1072. SP179–60.
- [62] ACI Committee 233, Slag Cement in Concrete and Mortar (233R-03), American Concrete Institute, Farmington Hills, MI, 2003.
- [63] T. Fujii, A. Sugita, T. Ayano, Resistance to freezing and thawing of concrete with granulate blast furnace slag sand, in: Fifth International Conference on Construction Materials: Performance, Innovations and Structural Implications. Whistler, Canada, 2015.